Impact of the Sensor Temperature on Low Acetone Concentration Detection Using AlGaN/GaN HEMTs †

Ali Ahaitouf [1,2,*,‡] , **Yacine Halfaya** [3] , **Suresh Sundaram** [1,2] , **Simon Gautier** [3] , **Paul Voss** [1,4] , **Jean Paul Salvestrini** [1,2] and **Abdallah Ougazzaden** [1,4]

1   CNRS, Unité Mixte Internationale (UMI 2958), 2–3 rue Marconi, 57070 Metz, France; ssundara@georgiatech-metz.fr (S.S.); paul.voss@ece.gatech.ed (P.V.); Jean-Paul.Salvestrini@georgiatech-metz.fr (J.P.S.); abdallah.ougazzaden@georgiatech-metz.fr (A.O.)
2   Georgia Tech Lorraine, 2 rue Marconi, 57070 Metz, France
3   Institut Lafayette, 2 rue Marconi, 57070 Metz, France; yacine.halfaya@institutlafayette.eu (Y.H.); simon.gautier@institutlafayette.eu (S.G.)
4   Georgia Institute of Technology, School of Electrical and Computer Engineering, GT-Lorraine, 57070 Metz, France
*   Correspondence: ali.ahaitouf@georgiatech-metz.fr
†   Presented at the 7th Electronic Conference on Sensors and Applications, 15–30 November 2020; Available online: https://ecsa-7.sciforum.net/.
‡   Permanent address: Faculté des Sciences et Techniques, Laboratoire SIGER, Université Sidi Mohammed Ben Abdellah, B.P. Fès 2202, Morocco; ali.ahaitouf@usmba.ac.ma

Abstract: In this work, we report on AlGaN/GaN HEMT sensors for acetone concentration below 100 ppm and in a broad range of the sensor temperature varying from RT to 300 °C. At RT, in the presence of acetone, a smooth and monotonic decrease of the current is observed with a rather large response of 15 µA/ppm and with a large response time (several minutes) and memory effect. At a high temperature (300 °C), a current decrease is first observed just after the acetone injection, then followed by an increase, which saturates and stabilizes at a constant value. In order to clarify this unexpected behaviour, a detailed study of the sensor response versus the temperature and acetone injection flow is carried out. The outcome of this investigation is that a competition between the current variations induced by both the sensor and gas flow temperature difference from one side and the acetone dipolar moment from the other side can explain this transient. Our study highlights that AlGaN/GaN HEMT-based sensors allow for very sensitive acetone detection at both room and high temperatures. Nevertheless, care must be taken during the characterization and operation of such sensors especially at high operating temperatures. On the other hand, the high temperature operation helps to improve the sensor response and suppress the memory effect.

Keywords: HEMT; AlGaN/GaN; acetone; temperature; drain current; sensor; sensing; transistor

1. Introduction

With the recent progress in biomedicine and biosensors, in environmental and industrial control, acetone detection emerges as a huge challenge to be met with small, wearable and less expensive sensors. In fact, acetone is one of the important volatile organic compounds (VOCs) used as a biomarker of several diseases [1] and is widely used in research laboratories and biochemical industries. Modern electronic devices, with their reduced sizes and fast time response can play a major role in this field of sensing.

AlGaN/GaN HEMTs have been shown to be efficient sensors for a broad range of physical parameters, in either liquid or dry condition, such as pressure sensors [2,3], gas detection [4,5],

pH sensors [6] and, more recently, used as biosensors for the rapid detection of viruses [7]. These achievements could pave the way for the use of these HEMT transistors in electronic nose development, particularly useful for VOC detection. In the acetone case, sensors with responsivity in the range below 1 ppm are desired [1].

Pioneering works on chemical and gas sensing using AlGaN/GaN HEMTs started at the beginning of the 2000s [8–11]. Neuberger et al. reported on polar liquid sensing at room temperature using a gate-less HEMT. They tested both acetone, propanol and methanol in the liquid phase and showed that, whatever the polar liquid, the drain current decreased from its clean air value to a lower value in the presence of acetone. The same trend was reported by Mehandru et al. [11]. They used the AlGaN/GaN HEMT to measure acetone and alcohol effects, and the sensing mechanism was attributed to the interaction between the dipole moments and the 2D gas. However, the magnitude of the changes did not correlate with the dipole moment of the liquids, suggesting that steric hindrance effects or the mismatch orientation of the adsorbed molecules should play a role in the detection mechanism [10]. HEMT-based sensing of acetone in the gaseous phase was also tested by Sun et al. [12]. For that, they used a WO_3 gated AlGaN/GaN HEMT integrated with a micro-heater allowing the operation of the HEMT at a temperature higher than 200 °C. In contrast to the previously cited studies, they observed a large increase of the drain current of the HEMT in the presence of acetone.

In this work, in an attempt to elucidate the reason for the discrepancies in the sensor response to acetone in the gaseous phase, we report on a Pt-gated AlGaN/GaN HEMT sensor for acetone concentration ranging from 30 to 150 ppm and for operating temperatures varying from room temperature up to 300 °C.

2. Device Fabrication and Measurement Setup

The AlGaN/GaN heterostructure was grown by metal organic vapour phase epitaxy (MOVPE) on a semi-insulating GaN template on a sapphire substrate using trimethylgallium (TMGa), trimethylaluminium (TMAl) and ammonia (NH_3) as the gallium, aluminium and nitrogen sources, respectively. The epilayers consisted of a 260 nm thick undoped GaN layer and a 19 nm thick undoped AlGaN layer with an aluminium (Al) composition of 30%, which was verified by XRD measurements. AFM measurements showed a smooth surface with an RMS roughness of 0.8 nm. For the sensor fabrication, source and drain contacts were defined by optical lithography. Using an electron beam evaporator, the ohmic contact was achieved by the multilayer 12/200/40/100 nm Ti/Al/Ni/Au deposition followed by a rapid thermal annealing at 870 °C for 30 s under a nitrogen atmosphere. Rectangular-shaped gates were defined by optical lithography, and the platinum (Pt) contact was evaporated with a thickness of 15 nm followed by lift-off to obtain 16 sensors on a single chip with a size of 3 mm^2 (see Figure 1).
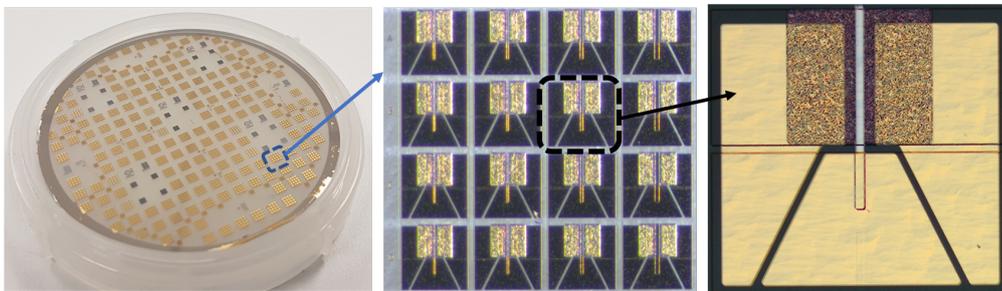

Figure 1. (Left) Photograph of a two inch wafer processed HEMT acetone sensor. (Middle) single ship of 16 sensors. (Right) SEM image showing a single HEMT sensor.

For gas sensing, the sensors were placed in a closed chamber and electrically connected to a source measurement unit for device polarization and current measurements. The acetone flow was

prepared by bubbling a controlled carrier flow of nitrogen in a bubbler containing the solvents in the liquid phase and carried out to the chamber.

3. Sensing Mechanism

The acetone sensing mechanism using a AlGaN/GaN HEMT device was described by Rabba and Stien [13]. The drain current can be described by:

$$I_{DS} = W \times q \times v_{drift} \times N_s(m), \tag{1}$$

where W is the gate width, v_{drift} is the channel position-dependent electron drift velocity, $N_s(m)$ is the charge density in the transistor channel and m is the Al mole fraction in the AlGaN layer. The expression of this sheet density is obtained by solving the 1D Poisson's equation given by:

$$N_s(m) = \frac{\epsilon_o \epsilon_r(m)}{q \times d} \times \left(V_{GS} + \Delta V - v_{th} - V_{DS} - \frac{E_F(m)}{q} \right), \tag{2}$$

where $\epsilon_r(m) = 9.5 - 0.5m$ is the dielectric constant of the $Al_m Ga_{1-m} N$, q is the electronic charge, d is the thickness of the AlGaN layer, V_{GS} is the gate voltage, V_{DS} is the drain–source voltage, $E_F(m)$ is the Fermi level energy with respect to the GaN conduction band, m is the aluminium composition and v_{th} is the threshold voltage of the HEMT, which is negative for a normally-on HEMT. ΔV corresponds to the potential variation induced by the acetone molecule dipole calculated using the Helmholtz condenser model and given by:

$$\Delta V = \frac{N_{sp} \times p \times cos\theta}{\epsilon_o \times \epsilon_r}, \tag{3}$$

where N_{sp} is the dipole density per unit area, p is the dipole moment of the polar molecule in Debye (D), θ is the angle between the dipole moment vector and the surface normal, ϵ_r is the relative permittivity of the gas and ϵ_o is the vacuum permittivity.

For normally-on HEMT, the 2D electron gas induces positive charges on the gate, which attract and trap the acetone molecular dipoles, leading to a depletion of the 2D gas and thus a current decrease (see Figure 2). This corresponds to an induced negative ΔV, in Equation (2).
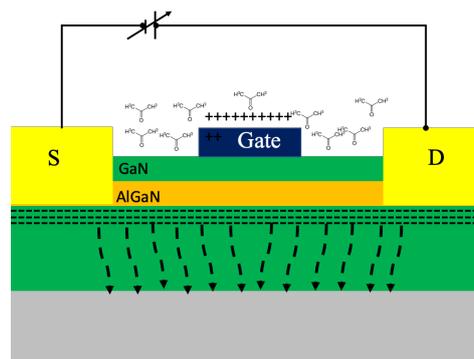

Figure 2. Sketch of the operation principle of an HEMT for acetone sensing.

4. Results

4.1. Room Temperature Measurements

Figure 3 shows the typical time dependence of the induced drain current variation, ΔI_{DS}, when the gas flow is switched from pure $N_2(200 \text{ cm}^3)$ to acetone diluted in N_2 at a concentration of 60 ppm and then to pure N_2. A sharp decrease of the current is observed just after the acetone switching. The current then stabilizes for a few seconds (see the inset of Figure 3), starts to decrease again with a smaller slope and finally saturates to reach a constant value. When the gas flow is switched back to

pure N_2, a slow increase of the current followed by a saturation without full recovering is observed. Note that a full recovery is obtained after a few hours of operation.
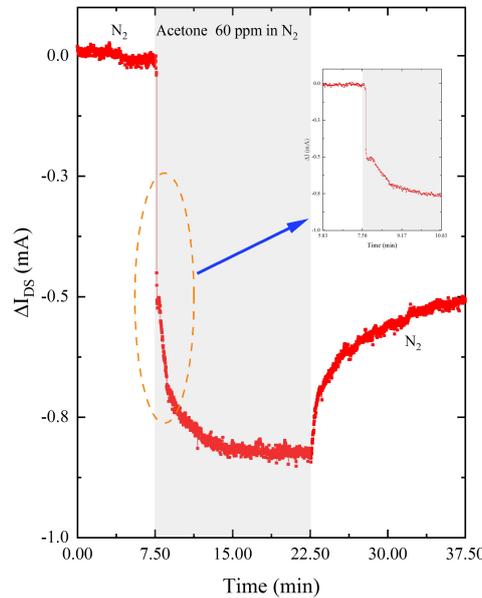

Figure 3. Typical time dependence of the induced drain current variation, ΔI_{DS}, when the gas flow is switched from pure N_2 (200 cm^3) to acetone diluted in N_2 at a concentration of 60 ppm, then to pure N_2. Measurements were carried out at room temperature and at a bias polarisation V_{DS} of 5 V.

The sensitivity ($S = \frac{I_{DS,acetone} - I_{DS,N_2}}{\Delta C} = \frac{\Delta I_{DS}}{\Delta C}$), relative variation ($\frac{\Delta I_{DS}}{I_{DS}} = \left| \frac{I_{DS,acetone} - I_{DS,N_2}}{I_{DS,N_2}} \right|$) and response time (10% to 90% of the total induced current variation) of the sensor were derived from the data of Figure 3. The sensitivity, relative sensitivity and response time were equal to 15 µA/ppm, 2.4% and 131 s, respectively. Table 1 summarizes the values of this set of characteristics obtained for different acetone concentrations.

Table 1. Values of the sensitivity $S = \frac{I_{DS,acetone} - I_{DS,N_2}}{\Delta C} = \frac{\Delta I_{DS}}{\Delta C}$, relative variation $\frac{\Delta I_{DS}}{I_{DS}} = \left| \frac{I_{DS,acetone} - I_{DS,N_2}}{I_{DS,N_2}} \right|$ and response time of the HEMT sensor at room temperature and for different concentrations.

N_2 Flow (cm^3/s)	Acetone Concentration (ppm)	$\frac{\Delta I}{\Delta C}$ (µA/ppm)	$\frac{\Delta I}{I}$ (%)	Response Time (s)
100	30	33.3	2.7	70
200	60	15	2.4	131
300	90	7	1.7	166
400	120	6	1.9	150

A large decrease of the sensitivity is observed when the acetone concentration is increased from 30 to 120 ppm. Such behaviour cannot be explained by a saturation of the current variation due to a memory effect because each measurement started only after a full recovery of the sensor. A possible reason for this unexpected decrease of the sensor performance is a cooling of the sensor by the gas flow. When the gas flow is introduced into the chamber, the temperature of the sensor decreases and reaches a minimum before increasing when the equilibrium is reached in the chamber. This transient cooling of the sensor induces a current transient, which might partially compensate for the decrease of the current induced by the acetone, leading to the behaviour shown in the inset of Figure 3. The transient cooling of the sensor becomes larger when the acetone concentration is increased since the gas flow is increased correspondingly. This assumption is supported by data reported recently by Sun et al. [12] who reported a low sensitivity of 0.3 µA/ppm for acetone in air at 300 °C, conditions for which the gas flow cooling might play a large role. The increase of the response time with the increase of acetone

concentration could also be explained by the transient cooling, which affects mainly the saturation region of the sensor response and thus the time at which 90% of the response is reached.

4.2. High Temperature Measurements

To explore the effect of the cooling transient on the sensor response, we performed acetone sensing at a higher temperature up to 300 °C, for which larger cooling transients are expected, and for different exposure times of the sensor to the acetone flow. Results obtained at 300 °C for an acetone concentration of 60 ppm and a time exposure varying from 30 s to 120 s are reported in Figure 4a–d.
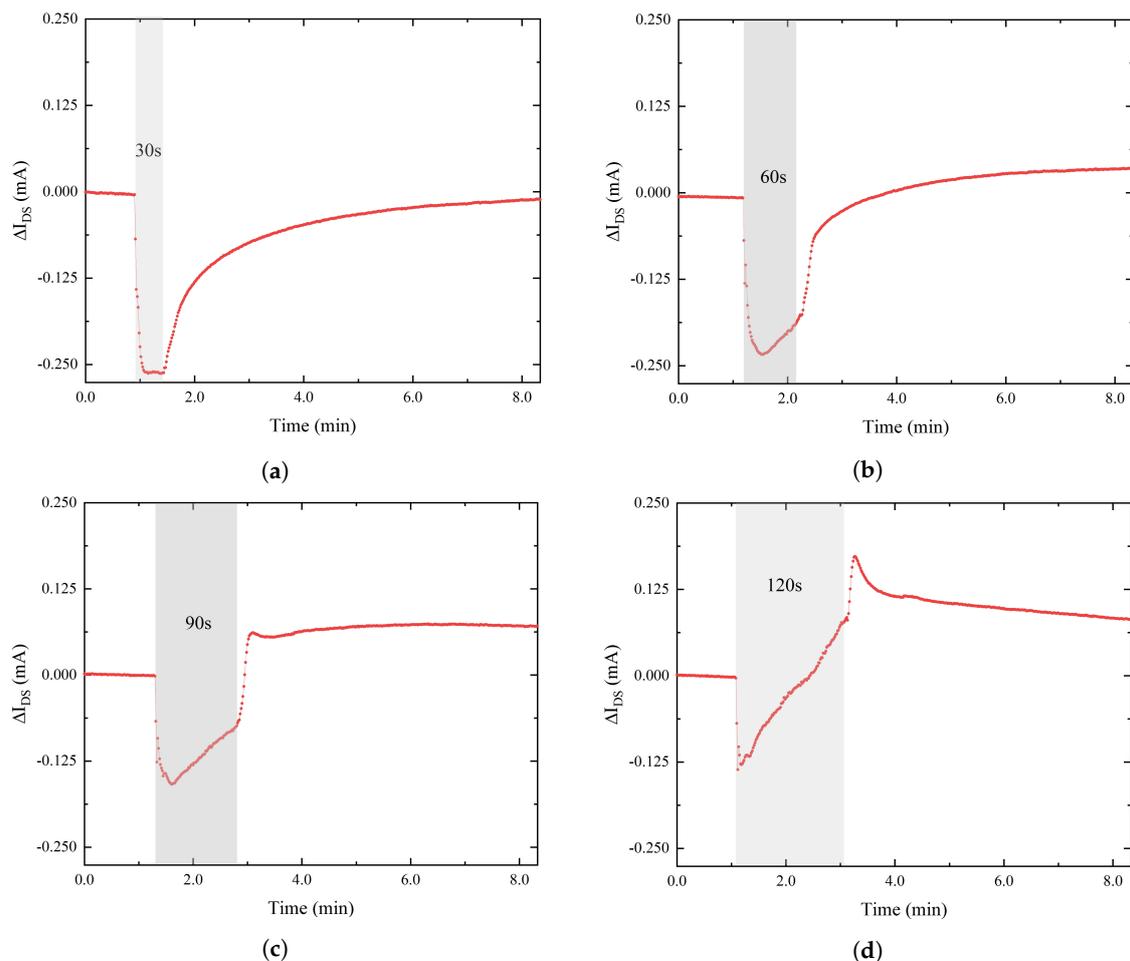

Figure 4. Typical time dependence of the induced drain current variation, ΔI_{DS}, when the gas flow is switched from pure N_2 (200 cm^3) to acetone diluted in N_2 at a concentration of 60 ppm, then to pure N_2 for different time exposures varying from 30 s (a), 60 s (b), 90 s (c) and 120 s (d). Measurements were carried out at 300 °C and at a bias polarisation V_{DS} of 5 V.

Fort the shortest exposure time, a sharp and fast decrease of the current is observed just after the acetone switching. Then, the current variation saturates and reaches a constant value. When the gas flow is switched back to pure N_2, a slow increase of the current followed by a saturation with a full recovery is observed. The sensitivity, relative variation and response time were equal to 4.2 μA/ppm, 1.9% and 6 s, respectively. As expected, the sensor response and the recovery time were smaller at a high temperature than at room temperature. Nevertheless, note that the sensitivity is almost four times smaller than that obtained at room temperature. This is likely due to the transient cooling effect, which partially compensates for the acetone induced current decrease. For a longer exposure time, the cooling of the sensor by the gas flow increases, while the compensation effect increases. A larger current increase due to the cooling occurs, leading to an effective sensitivity decrease. This cooling

induced current increase extends after the switching to pure N$_2$ gas and then slowly decreases before reaching the initial current value (not shown here). For a long exposure time, there is thus a strong competition between the current decrease due to the acetone interaction with the gate and the current increase due to the sensor cooling by the gas flow. As shown in Figure 5, for a very long exposure time (30 min), the sensor cooling effect on the current becomes fully dominant and completely hides the acetone response.
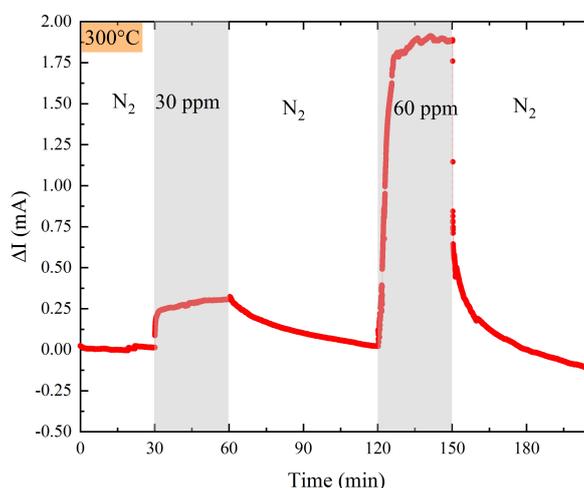

Figure 5. Typical time dependence of the induced drain current variation, ΔI_{DS}, when the gas flow is switched from pure N_2 (100 cm^3) to acetone diluted in N_2 at a concentration of 30 ppm for 30 min, then to pure N_2, then to acetone diluted in N_2 at a concentration of 60 ppm for 30 mn and finally to pure N_2. Measurements were carried out at 300 °C and at a bias polarisation V_{DS} of 5 V.

5. Conclusions

At room temperature, in the presence of acetone, a smooth and monotonic decrease of the HEMT sensor current is observed with a rather large sensitivity, but with a slow response time and a very long recovering time. The sensor response is in agreement with the electrostatic interaction between the 2D gas of the HEMT with the dipolar moment of the acetone molecules. At a high temperature (300 °C), a cooling effect due the gas flow, which counter balances the acetone response, is observed. This cooling effect becomes dominant for a long exposure time of the sensor to acetone gas flow and can completely hide the sensor response to acetone. AlGaN/GaN HEMT-based sensors are shown to allow for very sensitive acetone detection at both room and high temperatures. Nevertheless, care must be taken during the characterization and operation of such sensors especially at high operating temperatures. Increasing the latter can help to improve the response and recovery time, but requires the control or cancellation of the current transient due to the cooling of the sensor by the gas flow.

Author Contributions: Conceptualisation, measurements, writing, original draft preparation, methodology: A.A.; Software, methodology, devices processing: Y.H.; Devices growth: S.S.; Resources: S.G.; Discussion, methodology: P.V.; Methodology, writing, review and editing: J.P.S.; Supervision, project administration, funding acquisition, review and editing: A.O.

Conflicts of Interest: The authors declare no conflict of interest

References

1. Wilson, A. Advances in Electronic-Nose Technologies for the Detection of Volatile Biomarker Metabolites in the Human Breath. *Metabolites* **2015**, *5*, 140–163. doi:10.3390/metabo5010140.

2. Kang, B.S.; Kim, S.; Kim, J.; Mehandru, R.; Ren, F.; Baik, K.; Pearton, S.J.; Gila, B.P.; Abernathy, C.R.; Pan, C.C.; et al. AlGaN/GaN high electron mobility transistor structures for pressure and pH sensing. *Phys. Status Solidi (C)* **2005**, *2*, 2684–2687. doi:10.1002/pssc.200461269.

3. Gajula, D.; Jahangir, I.; Koley, G. High Temperature AlGaN/GaN Membrane Based Pressure Sensors. *Micromachines* **2018**, *9*, 207. doi:10.3390/mi9050207.

4. Bishop, C.; Halfaya, Y.; Soltani, A.; Sundaram, S.; Li, X.; Streque, J.; Gmili, Y.E.; Voss, P.L.; Salvestrini, J.P.; Ougazzaden, A. Experimental Study and Device Design of NO, NO_2, and NH_3Gas Detection for a Wide Dynamic and Large Temperature Range Using Pt/AlGaN/GaN HEMT. *IEEE Sens. J.* **2016**, *16*, 6828–6838. doi:10.1109/jsen.2016.2593050.

5. Halfaya, Y.; Bishop, C.; Soltani, A.; Sundaram, S.; Aubry, V.; Voss, P.; Salvestrini, J.P.; Ougazzaden, A. Investigation of the Performance of HEMT-Based NO, NO_2 and NH_3 Exhaust Gas Sensors for Automotive Antipollution Systems. *Sensors* **2016**, *16*, 273. doi:10.3390/s16030273.

6. Sama, N.Y.; Bouhnane, H.; Gautier, S.; Ahaitouf, A.; Matray, J.M.; Salvestrini, J.P.; Ougazzaden, A.; Hathcock, A.; He, D.; Vuong, T.Q.P.; et al. Investigation of Sc2O3 Based All-Solid-State EIS Structure for AlGaN/GaN HEMT pH Sensor. In Proceedings of the 2019 IEEE SENSORS, Montreal, QC, Canada, 27–30 October 2019. doi:10.1109/sensors43011.2019.8956762.

7. Yang, J.; Carey, P.; Ren, F.; Mastro, M.A.; Beers, K.; Pearton, S.J.; Kravchenko, I.I. Zika virus detection using antibody-immobilized disposable cover glass and AlGaN/GaN high electron mobility transistors. *Appl. Phys. Lett.* **2018**, *113*, 032101. doi:10.1063/1.5029902.

8. Kao, K.W.; Hsu, M.C.; Chang, Y.H.; Gwo, S.; Yeh, J.A. A Sub-ppm Acetone Gas Sensor for Diabetes Detection Using 10 nm Thick Ultrathin InN FETs. *Sensors* **2012**, *12*, 7157–7168. doi:10.3390/s120607157.

9. Neuberger, R.; Müller, G.; Ambacher, O.; Stutzmann, M. High-Electron-Mobility AlGaN/GaN Transistors (HEMTs) for Fluid Monitoring Applications. *Phys. Status Solidi (A)* **2001**, *185*, 85–89. doi:10.1002/1521-396x(200105)185:1<85::aid-pssa85>3.0.co;2-u.

10. Pearton, S.J.; Kang, B.S.; Kim, S.; Ren, F.; Gila, B.P.; Abernathy, C.R.; Lin, J.; Chu, S.N.G. GaN-based diodes and transistors for chemical, gas, biological and pressure sensing. *J. Phys. Condens. Matter* **2004**, *16*, R961–R994. doi:10.1088/0953-8984/16/29/r02.

11. Mehandru, R.; Luo, B.; Kang, B.; Kim, J.; Ren, F.; Pearton, S.; Pan, C.C.; Chen, G.T.; Chyi, J.I. AlGaN/GaN HEMT based liquid sensors. *Solid-State Electron.* **2004**, *48*, 351–353. doi:10.1016/s0038-1101(03)00318-6.

12. Sun, J.; Sokolovskij, R.; Iervolino, E.; Santagata, F.; Liu, Z.; Sarro, P.M.; Zhang, G. Characterization of an Acetone Detector Based on a Suspended WO3-Gate AlGaN/GaN HEMT Integrated With Microheater. *IEEE Trans. Electron Devices* **2019**, *66*, 4373–4379. doi:10.1109/ted.2019.2936912.

13. Rabbaa, S.; Stiens, J. Validation of a triangular quantum well model for GaN-based HEMTs used in pH and dipole moment sensing. *J. Phys. D Appl. Phys.* **2012**, *45*, 475101. doi:10.1088/0022-3727/45/47/475101.